38. Siliprandi R, Canella R, Carmignoto G, et al. N-methyl-D-aspartate-induced neurotoxicity in the adult rat retina. *Vis Neurosci.* 1992; 8:567–573.
39. Jeon CJ, Strettoi E, Masland RH. The major cell populations of the mouse retina. *J Neurosci.* 1998;18:8936–8946.
40. Onozuka T, Sawamura D, Goto M, Yokota K, Shimizu H. Possible role of endoplasmic reticulum stress in the pathogenesis of Darier's disease. *J Dermatol Sci.* 2006;41:217–220.
41. Weil M, Jacobson MD, Coles HS, et al. Constitutive expression of the machinery for programmed cell death. *J Cell Biol.* 1996;133: 1053–1059.
42. Taylor J, Gatchalian CL, Keen G, Rubin LL. Apoptosis in cerebellar granule neurones: involvement of interleukin-1 beta converting enzyme-like proteases. *J Neurochem.* 1997;68:1598–1605.
43. Inokuchi Y, Shimazawa M, Nakajima Y, Suemori S, Mishima S, Hara H. Brazilian green propolis protects against retinal damage in vitro and in vivo. *Evid Based Complement Alternat Med.* 2006;3:71–77.
44. Chidlow G, Wood JP, Manavis J, Osborne NN, Casson RJ. Expression of osteopontin in the rat retina: effects of excitotoxic and ischemic injuries. *Invest Ophthalmol Vis Sci.* 2008;49:762–771.
45. Sucher NJ, Lipton SA, Dreyer EB. Molecular basis of glutamate toxicity in retinal ganglion cells. *Vision Res.* 1997;37:3483–3493.
46. Henneberry RC, Novelli A, Cox JA, Lysko PG. Neurotoxicity at the N-methyl-D-aspartate receptor in energy-compromised neurons. An hypothesis for cell death in aging and disease. *Ann NY Acad Sci.* 1989;568:225–233.
47. Uehara T, Nakamura T, Yao D, et al. S-nitrosylated protein-disulphide isomerase links protein misfolding to neurodegeneration. *Nature.* 2006;441:513–517.
48. Wang XZ, Lawson B, Brewer JW, et al. Signals from the stressed endoplasmic reticulum induce C/EBP-homologous protein (CHOP/GADD153). *Mol Cell Biol.* 1996;16:4273–4280.
49. Ubeda M, Habener JF. CHOP gene expression in response to endoplasmic-reticular stress requires NFY interaction with different domains of a conserved DNA-binding element. *Nucleic Acids Res.* 2000;28:4987–4997.
50. Foti DM, Welihinda A, Kaufman RJ, Lee AS. Conservation and divergence of the yeast and mammalian unfolded protein response. Activation of specific mammalian endoplasmic reticulum stress element of the grp78/BiP promoter by yeast Hac1. *J Biol Chem.* 1999;274:30402–30409.

Current Eye Research, 33:247–252, 2008

ISSN: 0271-3683 print / 1460-2202 online
DOI: 10.1080/02713680801919716

informa
healthcare

The Efficacy of TonoLab in Detecting Physiological and Pharmacological Changes of Mouse Intraocular Pressure–Comparison with TonoPen and Microneedle Manometery

Tadashiro Saeki,
Makoto Aihara,
Masaaki Ohashi,
and Makoto Araie
Department of Ophthalmology, University of Tokyo School of Medicine, Tokyo, Japan

ABSTRACT *Purpose*: The efficacy of two non-invasive tonometers, TonoLab and TonoPen XL, in detecting physiological or pharmacological changes of intraocular pressure (IOP) in mouse eyes, was assessed by comparison with a microneedle method. *Material and Methods:* C57BL6 mice, bred under the 12-hr light and dark cycle over 2 weeks, were used. Under systemic anesthesia, mouse eyes were cannulated by a microneedle connected to a transducer and a water reservoir. We manipulated the intracameral pressure by changing the reservoir height, and obtained tonometer readings at each pressure ($n = 39$) with TonoLab and TonoPen XL. The correlation between each tonometer and the manometer was analyzed. Then the diurnal variation of IOP in the light and dark phases, and the IOP-lowering effect at 2 hr after latanoprost instillation, were measured with TonoLab, TonoPen XL, and a microneedle tonometer ($n = 8$). *Results:* In mouse eyes, TonoPen XL could not show reliable scores, but TonoLab readings showed a strong correlation with manometer readings ($y = 0.87x - 0.27$, $r^2 = 0.917$). Nocturnal elevation of IOP in mouse eyes was significantly indicated with TonoLab and a microneedle tonometer ($p < 0.001$), but not with TonoPen XL. Latanoprost significantly reduced IOP by 2.1 ± 2.8 and 2.0 ± 1.0 mmHg with TonoLab and a microneedle tonometer, but not with TonoPen XL. *Conclusion:* TonoLab provides similar readings to a microneedle tonometer, and diurnal variation and drug effect were detectable in mouse eyes. TonoLab promises to be a non-invasive and useful method to evaluate physiological and pharmacological studies in mouse eyes.

KEYWORDS diurnal variation; intraocular pressure; latanoprost; mouse; tonometer

Received 16 November 2007
Accepted 15 January 2008

Correspondence: Makoto Aihara, M.D., Ph.D., Department of Ophthalmology, University of Tokyo School of Medicine, 7-3-1 Hongo, Bunkyo-ku Tokyo 113-8655, Japan. E-mail: aihara-tky@umin.ac.jp

INTRODUCTION

Mouse models are well established in mimicking glaucoma and other conditions with high intraocular pressure (IOP) and in evaluating the IOP-lowering mechanism of drugs. They are easily bred at relatively low cost in a controlled

environment and are also amenable to genetic manipulation. To expand the possibility of using mouse eyes for glaucoma research, accurate and reproducible IOP measurement is indispensable. However, it is difficult to measure IOP in mice because of their small size. A direct measurement, using a microneedle cannulation into the anterior chamber connected to a transducer, can record intracameral pressure directly and with accuracy,[1–3] but this procedure is invasive, so it cannot be used at short intervals, and it carries a risk of infection or inflammation.

In recent years, some noninvasive and repeatable methods of measuring IOP in mice have been reported.[4–6] The TonoPen XL® electronic tonometer (TonoPen, Mentor, Santa Barbara, CA, USA) was the most popular noninvasive method.[5,7] There were many reports of IOP measurement in rat eyes using TonoPen, even in conscious rats, but it was originally designed for use in humans,[8] and it may be surmised that it will be less accurate in these small animals.[9] Special care was needed to avoid pushing the eyes in measurement, because it causes overestimation of the IOP.

Recently, the TonoLab® rebound tonometer (TonoLab, Tiolat, Helsinki, Finland) has become commercially available; it was the first tonometer designed for use in mice.[9] This instrument is small (handheld) and suitable for repeated use, and its lightweight probe makes it possible to make measurements with less artificial pressure. TonoLab readings are well related to manometric intracameral pressure.[7,10,11] Moreover, TonoLab has been found to be a valuable tool to evaluate mouse IOP, including the glaucoma model mouse DBA2J.[7] It is also more accurate than TonoPen.[10]

In mouse glaucoma models with high IOP, therefore, TonoLab may be more useful than TonoPen. However, mouse eyes, which show great promise in basic glaucoma research, require highly accurate IOP measurements to expand their usage possibilities. Thus far, the potential of these non-invasive tonometers in detecting physiological and pharmacological change of IOP has not been assessed.

In this study, TonoLab and TonoPen were used to measure IOP in mouse eyes in comparison with a microneedle manometer. Subsequently, the diurnal rhythm of intraocular pressure and the effect of topical latanoprost were assessed and compared among these instruments.

MATERIALS AND METHODS

Animals

Male C57BL6 mice (8 weeks old) were obtained from Saitama Jikken Dobutsu (Saitama, Japan). All mice were housed in clear plastic cages covered loosely with air filters and containing white pine shavings for bedding. All studies were in compliance with the Association for Research in Vision and Ophthalmology (ARVO) Resolution on the Use of Animals in Research, and also approved by local ethical committee for animal studies. The animals were entrained to a light schedule of alternating 12-hr periods of light and dark (12 L, 12 D, light on at 6:00 AM), with free access to food and water.

IOP Measurement

The mice were anesthetized by intraperitoneal injection of a mixture of ketamine (100 mg/kg) and xylazine (9 mg/kg), prepared at room temperature. Then topical 0.4% oxybuprocaine (Benoxyl®; Santen Pharmaceuticals, Osaka, Japan) was applied in both eyes before each experiment.

We used three instruments to measure IOP; the microneedle method, TonoPen, and TonoLab. Intraocular pressure was measured directly by the microneedle method in anesthetized mice as previously described.[1] Briefly, after loss of consciousness, the animal was placed in a restrainer that maintained a prone body position similar to awake mice and gently immobilized the head. The microneedle was connected to a pressure transducer, which relayed its signal to a bridge amplifier, and hence to an analogue-to-digital converter and computer. The microneedle tip was inserted through the cornea, and the data were automatically collected online into a computer database. To minimize variation in our measurements due to stress or physical activity, the IOP was measured under anesthesia. In addition, data were collected during a time window 4–6 min after injection of anesthetic during which IOP has been shown to plateau.[1]

With the TonoPen, values ranging from 6 mmHg to 69 mmHg were recorded without automatically averaged readings; we averaged 15 valid readings for one measurement. With the TonoLab, automatically averaged readings were recorded. When the statistical reliability of the average measurement, as represented by

the coefficient of variance of the measurement, was not minimal, the reading in both measurements with TonoPen and TonoLab was ignored and another measurement taken.

Manometric Calibration of the TonoPen and TonoLab

A glass microneedle (for mouse eyes) was inserted into the anterior chamber at the limbus of the right eye under a stereoscopic microscope, taking care to avoid lens injury. The absence of leakage around the needle was confirmed and corneal deformation was minimized by monitoring the intracameral pressure variation, as described below. The needle was connected to a three-way connector, which in turn was connected in parallel to a pressure transducer and a fluid reservoir (BSS Plus®; Alcon Laboratories, Fort Worth, TX, USA). The intracameral pressure could be increased or decreased by moving a fluid reservoir up or down while monitoring actual intracameral pressure with the pressure transducer. Calibration was performed using 8 eyes. In one eye, one pressure setting was performed every 5 mmHg between 5 mmHg and 30 mmHg. Thus, 5 pressures were set in one eye of 8 mice, in total 40 measurement settings.

The measurement of IOP with TonoPen or TonoLab was performed blind to the position of the reservoir and the transducer readings. Each measurement was plotted against the corresponding manometric values. Linear regression analyses were performed to obtain a mathematical formulation of the relationship between tonometric measurements and the manometric values.

Timeframe and the Order of Three Methods for IOP Measurements

IOP was measured using 8 mice for each method. Considering the pressure lowering by repeated IOP measurements, on the first day of experiments IOP was measured by TonoLab, and continuously measured by TonoPen with 30-min intervals. On the second day, IOP was measured by a microneedle method in the same timeframe. Considering the diurnal variation of IOP, all IOP measurements were finished within 1 hr in each day.

Diurnal Variation of IOP in Normal Mouse

IOP at 09:00 and 21:00 was measured in 8 mice with TonoLab, TonoPen, and the microneedle method. With TonoLab and TonoPen, IOP was measured in the same day in the same eyes, but with the microneedle, and one week's interval was allowed between the measurement at both times because of its penetration into the eye.

Effect of Topical Instillation of Latanoprost on Mouse IOP

We evaluated the effect of topical latanoprost (Xalatan; Pharmacia, Uppsala, Sweden) in 8 mouse eyes, using the three instruments, TonoLab, TonoPen, and the microneedle tonometer. At 16:00, latanoprost (0.005%, and 3 μl for mouse) was instilled into one randomly selected eye of each animal, and carrier solution was administered topically to the other eye as a control. General anesthesia was administered at 17:45. Two hours after instillation (18:00), IOP was measured in a masked manner. The ocular hypotensive effect was evaluated by comparison of the IOP between treated and untreated (contralateral) eyes.

Statistics

All data are shown as mean ± standard deviation. The difference between IOP measured at daytime and nighttime, and the difference between eyes treated with or without latanoprost, were statistically evaluated by means of a paired *t*-test.

RESULTS

TonoLab and TonoPen Measurement in Mouse Eyes (Fig. 1)

As shown in Figure 1B, the tip of the TonoPen was so large that, in the mouse, eye distortion and indentation of the globe or attachment of the tip to the eyelashes or lid were inevitable. In this study, a reliable score from TonoPen was not obtained in mouse eyes. Thus, only TonoLab was compared to the microneedle method.

Manometric Calibration of the TonoLab in Mouse Eyes (Fig. 2)

Calibration was performed at 5 pressure values per eye using 8 eyes. In practice, pressure settings were not

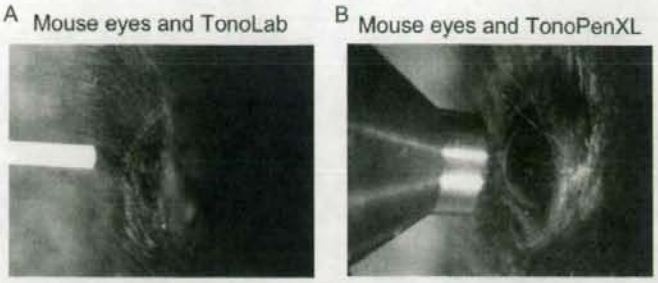

FIGURE 1 TonoLab and TonoPen measurement in mouse eyes. (A) The tip of TonoLab against mouse eyes. (B) The tip of TonoPen against mouse eyes. Note the diameter of both tips for eyeballs.

exact 5-mmHg intervals, as shown in Figure 2, and one measurement was failed. Thus, the total number became 39. A regression line was calculated by plotting TonoLab readings (39 different intracameral pressures) against the corresponding manometric values, and the formula, $y = 0.87x - 0.27$ was determined, where x represents the pressure measured with the pressure transducer and y represents the mean TonoLab readings. The correlation coefficient for TonoLab was $r^2 = 0.917$ (Fig. 2).

Diurnal Variation of IOP in Mouse (Fig. 3)

The mean IOP of the light phase was measured as 8.1 ± 0.6 and 9.8 ± 0.4 mmHg with TonoLab and the microneedle method, respectively ($n = 8$), with the mean IOP of the dark phase measuring 15.4 ± 2.1 and 18.4 ± 0.7 mmHg. There were significant IOP differences between the light- and dark-phase IOPs measured with TonoLab (8.1 ± 0.6 vs. 15.4 ± 2.1, $p = 0.012$ by paired t-test), and the microneedle method (9.8 ± 0.4 vs. 18.4 ± 0.7, $p < 0.001$ by paired t-test).

Effect of Topical Instillation of Latanoprost on Mouse IOP (Fig. 4)

Using TonoLab, the IOPs treated by carrier solution and latanoprost were measured as 12.5 ± 1.8 and 10.4 ± 2.0 mmHg ($p = 0.040$, paired t-test), respectively, and by the microneedle method as 14.4 ± 1.1 and 12.4 ± 1.4 mmHg ($p < 0.001$, paired t-test) ($n = 8$). The mean reductions in IOP shown by the two methods were 2.1 ± 2.8 and 2.0 ± 1.0 mmHg, respectively,

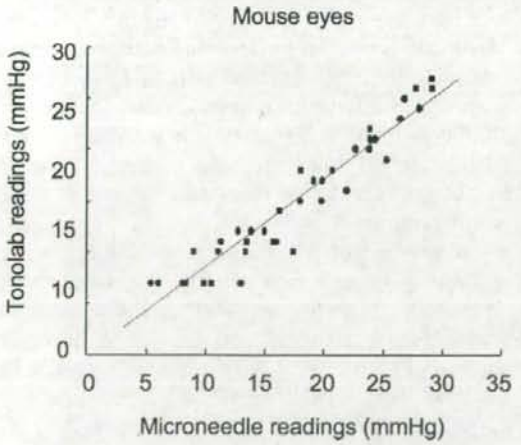

FIGURE 2 Calibration of the TonoLab and TonoPen XL in mouse eyes. Scatter diagram for TonoLab ($n = 39$) readings against the corresponding manometric values in mouse eyes. Regression line formula is $y = 0.87x - 0.27$ ($r^2 = 0.917$) for TonoLab.

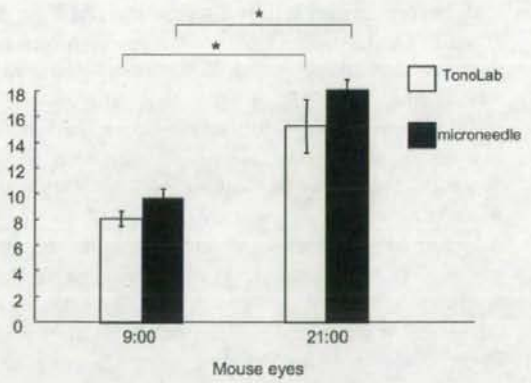

FIGURE 3 Circadian rhythm of IOP in normal mouse. IOP are measured at 9:00 AM and 9:00 PM with TonoLab (white column) and a microneedle (black column) in mouse eyes ($n = 8$). The data are the mean ± SD. *$p < 0.001$, by paired t-test.

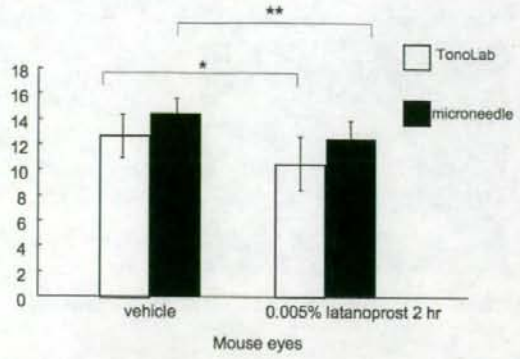

FIGURE 4 Effect of topical instillation of latanoprost on mouse IOP. IOP in both eyes was measured 2 hr after administration of latanoprost or vehicle with TonoLab (white column), and a microneedle (black column) in mouse eyes. The data are the mean ± SD. Asterisks indicate significance by paired *t*-test. * $p = 0.040$, ** $p < 0.001$.

and, with both, latanoprost significantly reduced IOP in mouse eyes ($p < 0.001$) (Fig. 4).

DISCUSSION

Recently, many rodent glaucoma models have been developed and characterized, but accurate IOP measurement with non-invasive instrumentation remained one of the most challenging tasks in such experiments. The TonoPen is widely used for rats and also used for mice among some investigators, but it requires a lot of training and experience for accurate and reproducible measurement in rat eyes, still more in mouse eyes. In our study, we were unable to obtain reliable scores in mouse eyes and finally abandoned the use of TonoPen for them. To date, TonoPen has been used in a few studies to measure high IOP in mouse glaucoma models such as DBA2J or other artificially modified mice,[12,13] but, recently, TonoLab has been used more in these glaucoma model mice.[7,14] This tendency underlines the difficulty in measuring rodent IOPs with TonoPen.

The tip of TonoPen is hard, and the tonometer itself is in direct contact with the eye. The effect of impact on the eye is thought incompatible with accurate measurements in glaucoma mouse models. As shown in Figure 1, the tip of the TonoPen is quite large against the mouse globe. Thus, with the globe in its natural position, a clean contact without pushing the eyeballs or contacting the eyelashes and lids was impossible to achieve. In contrast, the ultra-lightweight probe of the TonoLab needs to be ejected magnetically from the instrument only a few times to obtain a viable reading. The impact appears minimal compared with that of other instruments. In addition, it is possible to become proficient in this method without special training.

In this study, we compared the accuracy of TonoLab tonometers and a microneedle method in mice to assess their potential to detect the slight change of IOP in physiological diurnal variation or through treatment with ocular hypertensive agents. We found that TonoLab can detect these changes well in mouse eyes with some benefits. Of course, non-invasive measurement has some drawbacks, notably the lower accuracy of the IOP value compared to that measured by a microneedle.

IOP measurement with TonoLab, which can detect the diurnal changes, has a potential to clarify the molecular mechanisms of diurnal changes of IOP using normal or various kinds of transgenic mouse eyes. Already, diurnal variation of mouse IOP were different among the strains,[15] varied by light conditions,[16,17] and modified by a clock gene.[18] In these studies, diurnal variation of mouse IOP was measured by a microneedle method because TonoLab was not developed, although TonoPen had been already present. Our result suggests the potential use of TonoLab for future studies, additionally, considering diurnal changes are important to development of ocular hypotensive drugs, or to clarify the mechanism of IOP reduction. For example, IOP-lowering effect by prostaglandin analogues was obviously higher in the nighttime than that in the daytime.[19] Thus, drug screening considering diurnal variation of IOP is more effective and important in mouse eyes. Moreover, non-invasive measurement of IOP with TonoLab is repeatable in the same eye with a short interval compared to the invasive microneedle method, which leads to reduce the number of experimental animals.

Moreover, repeated measurement in the same eye permits easy detection of the effect of drugs such as beta-blockers affecting the IOP in the contralateral eye through systemic circulation following absorption through the mucosal tissue. This cannot be evaluated by an invasive microneedle method. Also, TonoLab can be used in the awake mice. Thus, IOP may be evaluated in more physiological conditions compared to that under anesthesia.

Taken together, TonoLab is a significant advance and convenient instrument for use in small animal

eyes. Therefore, our study to indicate the usefulness of TonoLab for the measurement of physiological or pharmacological changes in mouse IOP may be worth expanding the application of mouse eyes for glaucoma studies.

ACKNOWLEDGMENTS

Supported in part by grants H18-Kankakuippan-001 from the Ministry of Health, Labor, and Welfare of Japan, and A18209053 from the Ministry of Education, Culture, Sports, Science, and Technology of Japan.

REFERENCES

[1] Aihara M, Lindsey JD, Weinreb RN. Reduction of intraocular pressure in mouse eyes treated with latanoprost. *Invest Ophthalmol Vis Sci*. 2002;43:146–150.

[2] Avila MY, Carre DA, Stone RA, Civan MM. Reliable measurement of mouse intraocular pressure by a servo-null micropipette system. *Invest Ophthalmol Vis Sci*. 2001;42:1841–1846.

[3] John SW, Hagaman JR, MacTaggart TE, Peng L, Smithes O. Intraocular pressure in inbred mouse strains. *Invest Ophthalmol Vis Sci*. 1997;38:249–253.

[4] Cohan BE, Bohr DF. Measurement of intraocular pressure in awake mice. *Invest Ophthalmol Vis Sci*. 2001;42:2560–2562.

[5] Reitsamer HA, Kiel JW, Harrison JM, Ransom NL, McKinnon SJ. TonoPen measurement of intraocular pressure in mice. *Exp Eye Res*. 2004;78:799–804.

[6] Filippopoulos T, Matsubara A, Danias J, Huang W, Dobberfuhl A, Ren L, Mittag T, Miller JW, Grosskreutz CL. Predictability and limitations of non-invasive murine tonometry: Comparison of two devices. *Exp Eye Res*. 2006;83:194–201.

[7] Wang WH, Millar JC, Pang IH, Wax MB, Clark AF. Noninvasive measurement of rodent intraocular pressure with a rebound tonometer. *Invest Ophthalmol Vis Sci*. 2005;46:4617–4621.

[8] Midelfart A, Wigers A. Clinical comparison of the ProTon and TonoPen tonometers with the Goldmann applanation tonometer. *Br J Ophthalmol*. 1994;78:895–898.

[9] Dalke C, Pleyer U, Graw J. On the use of TonoPen XL for the measurement of intraocular pressure in mice. *Exp Eye Res*. 2005;80:295–296.

[10] Pease ME, Hammond JC, Quigley HA. Manometric calibration and comparison of TonoLab and TonoPen tonometers in rats with experimental glaucoma and in normal mice. *J Glaucoma*. 2006;15:512–519.

[11] Morris CA, Crowston JG, Lindsey JD, Danias J, Weinreb RN. Comparison of invasive and non-invasive tonometry in the mouse. *Exp Eye Res*. 2006;82:1094–1099.

[12] Gross RL, Ji J, Chang P, Pennesi ME, Yang Z, Zhang J, Wu SM. A mouse model of elevated intraocular pressure: Retina and optic nerve findings. *Trans Am Ophthalmol Soc*. 2003;101:163–169; discussion 169–171.

[13] Ueda J, Sawaguchi S, Hanyu T, Yaoeda K, Fukuchi T, Abe H, Ozawa H. Experimental glaucoma model in the rat induced by laser trabecular photocoagulation after an intracameral injection of India ink. *Jpn J Ophthalmol*. 1998;42:337–344.

[14] Danias J, Lee KC, Zamora MF, Chen B, Shen F, Filippopoulos T, Su Y, Goldblum D, Podos SM, Mittag T. Quantitative analysis of retinal ganglion cell (RGC) loss in aging DBA/2NNia glaucomatous mice: Comparison with RGC loss in aging C57/BL6 mice. *Invest Ophthalmol Vis Sci*. 2003;44:5151–5162.

[15] Savinova OV, Sugiyama F, Martin JE, Tomarev SI, Paigen BJ, Smith RS, John SW. Intraocular pressure in genetically distinct mice: An update and strain survey. *BMC Genet*. 2001;2:12.

[16] Aihara M, Lindsey JD, Weinreb RN. Twenty-four-hour pattern of mouse intraocular pressure. *Exp Eye Res*. 2003;77:681–686.

[17] Sugimoto E, Aihara M, Ota T, Araie M. Effect of light cycle on 24-hour pattern of mouse intraocular pressure. *J Glaucoma*. 2006;15:505–511.

[18] Maeda A, Tsujiya S, Higashide T, Toida K, Todo T, Ueyama T, Okamura H, Sugiyama K. Circadian intraocular pressure rhythm is generated by clock genes. *Invest Ophthalmol Vis Sci*. 2006;47:4050–4052.

[19] Ota T, Murata H, Sugimoto E, Aihara M, Araie M. Prostaglandin analogues and mouse intraocular pressure: Effects of tafluprost, latanoprost, travoprost, and unoprostone, considering 24-hour variation. *Invest Ophthalmol Vis Sci*. 2005;46:2006–2011.

Imaging Mouse Retinal Ganglion Cells and Their Loss In Vivo by a Fundus Camera in the Normal and Ischemia-Reperfusion Model

Hiroshi Murata,[1] Makoto Aihara,[2] Yi-Ning Chen,[2] Takashi Ota,[2] Jiro Numaga,[1] and Makoto Araie[2]

Purpose. To visualize retinal ganglion cells (RGCs) and their gradual loss in the living mouse.

Methods. With the use of B6.Cg-Tg(Thy1-CFP)23Jrs/J mice, which express cyan fluorescent protein (CFP) in RGCs, and a commercially available mydriatic retinal camera attached with a 5 million-pixel digital camera to visualize RGCs in vivo, the authors recorded fundus photographs longitudinally in the ischemia reperfusion model group and the untreated group to evaluate longitudinal changes in the number of RGCs in experimental models. Moreover, RGCs expressing CFP were evaluated histologically by a retrograde-labeling method and retinal whole mount or sections.

Results. The authors devised an in vivo imaging technique using a conventional retinal camera and visualized RGCs at the single-cell level. In the ischemia reperfusion model, a longitudinal reduction in the number of RGCs was demonstrated in each mouse eye. The number of RGCs and the fluorescence intensity of the nerve fiber decreased considerably during the first week. The percentages of RGCs decreased to 34.2% ± 7.5%, 24.1% ± 9.1%, 23.0% ± 9.3%, and 22.2% ± 8.4% (mean ± SD, $n = 5$) of the percentages before injury at 1, 2, 3, and 4 weeks after injury, respectively ($P < 0.001$). In this transgenic mouse, 97% of CFP-expressing cells were RGCs and 73% of RGCs expressed CFP.

Conclusions. This in vivo technique allows noninvasive, repeated, and longitudinal evaluation of RGCs for investigation of retinal neurodegenerative diseases and new therapeutic modalities for them. (*Invest Ophthalmol Vis Sci.* 2008;49:5546–5552) DOI:10.1167/iovs.07-1211

The neural retina and the optic disc are the only neuronal tissues that can be visualized in vivo without any invasive manipulation, and a great improvement has recently been achieved in imaging techniques for the evaluation of the human retina and optic nerve head (ONH).[1,2] Glaucoma, the second leading cause of vision loss in the world,[3] is associated with damage of optic nerve axons at the ONH and their cell bodies, the retinal ganglion cells (RGCs).[4] The only therapy available to stem RGC death in glaucoma is the reduction of intraocular pressure (IOP),[5] which is especially effective in patients with elevated IOP. However, elevated IOP is not the only pathogenic factor of glaucoma.[6]

Experimental neurodegenerative models such as ischemia reperfusion, optic nerve crush, intravitreal glutamate injection, and experimental ocular hypertension[7] have been used to investigate the pathogenesis of RGC death and possible neuroprotective treatment against it, for which reliable evaluation of the number of living RGCs was indispensable. As an experimental animal, the mouse has great advantages not only because it is less expensive and more easily handled than other animals but also because of the availability of various knockout or transgenic mice, enabling investigation of the role of a molecule in vivo. Until now, however, a technique allowing in vivo, noninvasive, and longitudinal observation of RGCs in the living mouse has not been established.

In the present study, we report a method of noninvasive visualization and quantitation of RGCs using B6.Cg-Tg(Thy1-CFP)23Jrs/J[8] mice. The strain expresses cyan fluorescent protein (CFP; major excitation peak, 433 nm; major emission peak, 475 nm),[9] in RGCs under the control of neuron-specific elements from the *Thy1* gene.[8] We evaluated longitudinal changes in the number of RGCs in the living mouse that underwent retinal ischemia reperfusion.[7]

Materials and Methods

Retinal Camera System

We used a commercially available mydriatic retinal camera (TRC-50IX; Topcon, Tokyo, Japan) attached with a 5 million-pixel digital camera (Nikon D1x; Nikon, Tokyo, Japan). The settings of the retinal camera were as follows: pupil, normal; image angle, 50°; flash, 300. The settings of the digital camera were as follows: shutter speed, 1/30 second; ISO, 800; image quality, fine. A 40-diopter aspherical lens (40D; Volk Optical, Mentor, OH) was fixed in front of the objective lens of the retinal camera at a distance of 5 mm, and the optical axis was adjusted. Built-in filters for fluorescein angiography were used for the fluorescein angiogram, band-pass filters, D436/20x (center wavelength, 436 nm; full width at half maximum [FWHM] transmission, 20 nm; Chroma Technology, Rockingham, VT), and BI0049 (center wavelength, 494 nm; FWHM transmission, 33 nm; Asahi Spectra, Tokyo, Japan) were used for the detection of CFP fluorescence. All images were captured with software (IMAGEnet; Topcon) and were saved by 3008 × 1960 × 8 bit-tagged image file format (TIFF). To improve the signal-to-noise ratio, a series of three images was taken for each measurement. The images were aligned automatically (AutoDeblur; Media-Cybernetics, Silver Spring, MD) and were combined (MaxIm DL 4.0; Diffraction Limited, Ontario, BC, Canada).

Ocular Fundus Photography

Three microliters of ophthalmic solution containing 0.5% tropicamide and 0.5% phenylephrine hydrochloride (Mydrin-P; Santen Pharmaceu-

From the [1]Tokyo Metropolitan Geriatric Hospital, Tokyo, Japan; and the [2]Department of Ophthalmology, University of Tokyo School of Medicine, Tokyo, Japan.

Supported in part by Grant H18-Kankakuippan-001 from the Ministry of Health, Labor, and Welfare of Japan and by Grant A18209053 from the Ministry of Education, Culture, Sports, Science and Technology of Japan (MAr).

Submitted for publication September 16, 2007; revised January 6, March 6, and June 25, 2008; accepted October 21, 2008.

Disclosure: **H. Murata**, None; **M. Aihara**, None; **Y.-N. Chen**, None; **T. Ota**, None; **J. Numaga**, None; **M. Araie**, None

The publication costs of this article were defrayed in part by page charge payment. This article must therefore be marked "*advertisement*" in accordance with 18 U.S.C. §1734 solely to indicate this fact.

Corresponding author: Makoto Aihara, Department of Ophthalmology, University of Tokyo School of Medicine, 7-3-1 Hongo, Bunkyo-ku Tokyo 113-8655, Japan; aihara-tky@umin.ac.jp.

tical, Osaka, Japan) was applied topically 10 minutes before anesthesia to dilate the pupil, and then mice were anesthetized with intraperitoneal injection of a mixture of ketamine (100 mg/kg body weight) and xylazine (9 mg/kg body weight). To avoid corneal injury, mice were restrained manually until they were anesthetized. A few minutes later, the mice were confirmed by the disappearance of the ciliary reflex to be fully anesthetized, and the cornea was covered carefully with mineral oil (Johnson's Baby Oil; Johnson & Johnson, New Brunswick, NJ) to prevent desiccation and to keep the surface smooth. Smoothness of the corneal surface and transparency were confirmed under an operation microscope. The laterality of the recorded eyes was chosen randomly. All the images were taken by an experienced investigator (HM).

Fluorescein Angiography

A 12-week-old C57BL/6 mouse was used. Ten microliters of fluorescein sodium (10% Fluorescite; Alcon Japan, Tokyo, Japan) was injected into the tail vein, and angiograms were obtained after 5 minutes. Fundus images were obtained using the retinal camera system, as described.

Animal Husbandry

Adult male and female B6.Cg-Tg(Thy1-CFP)23Jrs/J mice[8] were obtained from the breeding colony of The Jackson Laboratory (Bar Harbor, ME). The environment was kept at 23°C with a 12-hour light/12-hour dark cycle. All mice were fed ad libitum. Ten- to 15-week-old mice weighing 20 to 30 g were used. All studies were in compliance with the ARVO Statement for the Use of Animals in Ophthalmic and Vision Research.

Retrograde Labeling of RGCs in the Untreated Group and the Ischemia Reperfusion Group

To investigate the distribution of CFP in the retina, retrograde labeling with 1,1′-dioctadecyl-3,3,3′,3′-tetramethylindocarbocyanine perchlorate (DiI) was performed. Three B6.Cg-Tg (Thy1-CFP)23Jrs/J[8] mice were anesthetized and placed in a stereotactic frame. The skull was exposed and kept dry. Two holes were made at 2.92 mm behind the bregma in the anteroposterior axis and 0.5 mm lateral to the midline, and 5% DiI (1 μL at a rate of 0.5 μL/min; Molecular Probes, Eugene, OR) in dimethyl sulfoxide was injected at a depth of 2 mm from the brain surface into the superior colliculus of both sides. Ten days after injection, the mice were killed, and each eye was enucleated and fixed immediately in 4% paraformaldehyde in 0.1 M phosphate-buffered saline (PBS) for 30 minutes at 4°C. After the cornea and lens were removed, the sample was fixed again for 2 hours. Four radial relaxing incisions were made, the retina was prepared as a flattened whole mount on a glass slide with a coverslip, and an image was obtained with a fluorescence microscope (BX50; Olympus, Tokyo, Japan) with appropriate filters. Four square areas of 370 × 370 μm at a distance of approximately 1.5 mm from the optic nerve head were selected, and the number of cells was counted manually by an experienced investigator (MAi). Results were averaged for the four quadrant areas to obtain a value representing the eyes in question.

The same procedure was performed in the ischemia reperfusion group. Three weeks after ischemia reperfusion injury, DiI was injected into five mice of the ischemia reperfusion injury group. Seven days after injection, the retina was whole mounted. Then DiI^+ cells among CFP-expressing cells and CFP^+ cells among DiI^+ cells were counted and compared with those in untreated control eyes by an unpaired *t*-test. $P < 0.05$ was considered statistically significant.

Frozen Section

Localization of CFP^+ cells in the retina was assessed by retinal frozen sections. Four eyes of two thy1-CFP mice were enucleated, fixed in 4% paraformaldehyde in 0.1 M PBS for 1 hour, and fixed again for 1 hour after the removal of the cornea and lens. The globes were embedded (Tissue-Tek O.C.T.; Sakura Finetechnical, Tokyo, Japan) and cryopreserved in 15-mm-thick frozen sections, and sequential meridian sections (5-μm thick) were made through the optic disc. Sections were mounted on a glass slide with antifade medium containing propidium iodide (VectaShield with propidium iodide H-1300: Vector Laboratories, Burlingame, CA) to stain nuclei.

Comparison of a Mouse Fundus Photograph with a Whole Mount Retinal Image

Immediately after fundus photographs were obtained from a B6.Cg-Tg (Thy1-CFP) 23Jrs/J mouse,[8] the mouse was killed, and the retina was whole mounted and photographed with a fluorescence microscope (MZFLIII; Leica Microsystems Japan, Tokyo, Japan).

Ischemia Reperfusion Injury

Five mice were used for the ischemia reperfusion injury model.[10] Sodium pentobarbital (50 mg/kg body weight) was administered intraperitoneally. After anesthesia, the anterior chamber of the right eye was cannulated with a microneedle[11] connected to a reservoir filled with intraocular irrigating solution (BSS Plus; Santen Pharmaceutical). Retinal ischemia was induced by elevating the reservoir, and the IOP was raised to 110 mm Hg for 60 minutes.[12] During ischemia, the IOP was monitored continuously, the room temperature was maintained at 25°C,[13] and the room was kept dark. Ocular fundus images were recorded as described at five time points, just before injury and 1, 2, 3, and 4 weeks after it. Seven mice underwent sham operation by cannulation of the microneedle without elevation of the intracameral pressure and were used as controls. Their retinal images were recorded five times at 1-week intervals.

Reproducibility of Counting and Regional Difference of the Number of RGCs

We took fundus photographs of 10 eyes of five mice. Bilateral eyes of each mouse underwent fundus photography twice at intervals of 24 hours. The number of RGCs in the same area of the four square fields (220 × 220 pixels) was counted manually. Moreover, cell density was counted in each of four areas to investigate the regional differences of sampled area in each quadrant located 800 μm apart from the optic disc.

RGC Counting in Fundus Photographs and Retinal Flat Mount

Four square fields of 220 × 220 pixels (approximately 370 × 370 μm), one field from each quadrant of the retina, at a distance of approximately 800 μm from the optic nerve disc was always used for RGC counting in the fundus photograph or retinal flat mount, respectively. The number of cells emitting fluorescence was counted manually. Cell counting was performed by an experienced investigator (MAi) who was masked to the experimental treatment of the eye.

The numbers of RGCs counted in four square fields in the retina of ischemia reperfusion eyes were normalized to those obtained identically in the control eyes and were indicated as RGC survival rate. Each percentage is expressed in the text and figures as the mean ± SD. The difference in RGC density among four areas was statistically analyzed by a Kruskal-Wallis test. $P < 0.05$ was considered statistically significant.

Histologic Evaluation

After the last fundus photograph was taken at 4 weeks, one mouse was chosen randomly from the sham-operated control group and the ischemia reperfusion injury group. The mice were killed, and their eyes were enucleated, fixed in 4% paraformaldehyde and 2.5% glutaraldehyde in 0.1 M PBS for 1 hour, and fixed again for 24 hours after removal of the cornea and lens. The globes were processed to paraffin-embedded sections, and sequential meridian sections (5-μm thick) were made through the optic disc. Sections were stained with hematoxylin and eosin. Sections were examined with a light microscope (BX50; Olympus).

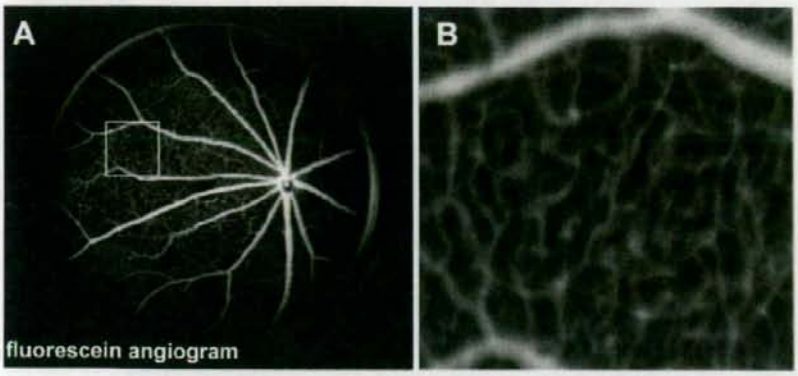

FIGURE 1. (A) Fluorescein angiogram of the mouse ocular fundus. (B) Area corresponding area to the *insert* in (A).

RESULTS

Mouse Fundus Photography

At first, to examine the resolving power of the fundus photograph with our method, we took a fundus fluorescein angiogram of a C57BL/6J mouse (Figs. 1A, 1B).

A wide area of retina was recorded, and blood capillaries were visualized with sufficient quality. Comparison of the fluorescein angiogram with those obtained from other studies suggested that the resolving power provided by our system was similar to that provided by a 10° view of a confocal scanning laser ophthalmoscope (cSLO) and superior to a 20° view of it,[14–16] whereas the area recorded by our system was similar to that provided by a 20° view of a cSLO.

Investigation of CFP Expression in the Mouse Retina

To identify the distribution of CFP in the B6.Cg-Tg(Thy1-CFP)23Jrs/J[8] mouse retina, retrograde labeling of RGCs with DiI was performed in five untreated eyes of three mice. Colo-

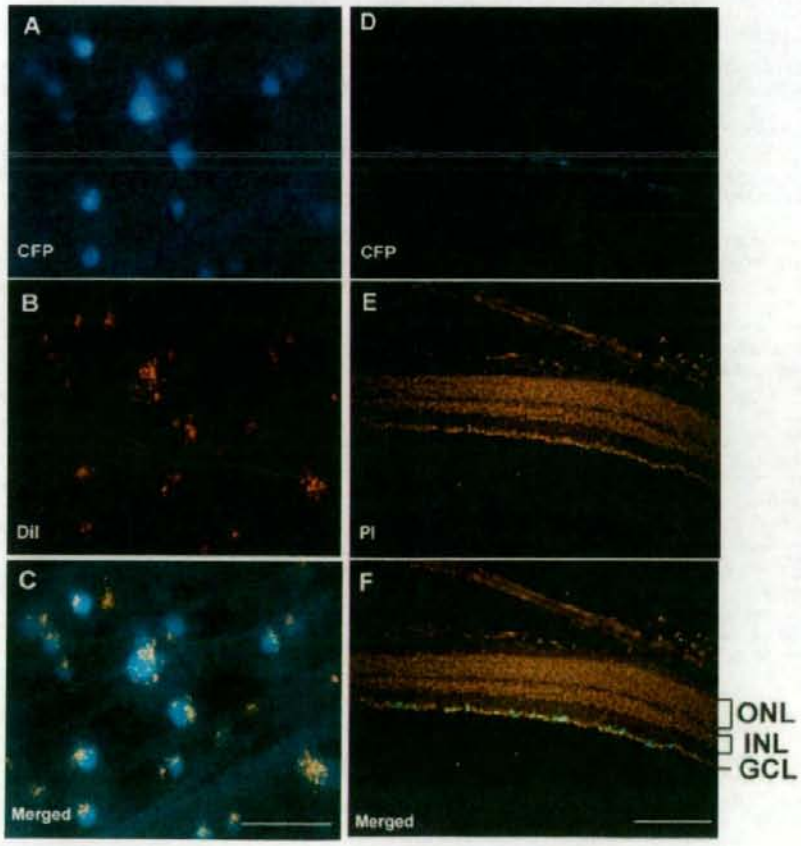

FIGURE 2. (A–C) Double labeling of RGCs with CFP and DiI. (A) RGCs expressing CFP. (B) Same field of DiI optics. (C) Merged image of (A) and (B). (D–F) Frozen section of Thy-1 CFP mouse. CFP was expressed only in the ganglion cell layer. Scale bars, (A–C) 50 μm; (D–F) 200 μm.

TABLE 1. Types of Labeling with CFP and DiI in Ischemia Reperfusion Group and Control Group

Cells	Control (%)	Ischemia Reperfusion (%)
DiI^+ among CFP^+	97.0	97.8
DiI^- among CFP^+	3.0	2.2
CFP^+ among DiI^+	72.6	59.2
CFP^- among DiI^+	27.4	40.8

calization of CFP and DiI in the same cells was observed (Figs. 2A–2C). Among the CFP^+ cells, DiI^+ cells accounted for 97.0% ± 2.7% (mean ± SD, $n = 5$) and DiI^- cells accounted for 3.0% ± 2.7%. Among the DiI^+ cells, CFP^+ cells accounted for 72.6% ± 5.2%, and CFP^- cells accounted for 27.4% ± 5.2% (Table 1). The density of DiI^+ cells was 2100 ± 136 cells/μm^2. Figures 2D–2F indicated that all the CFP^+ cells were localized only in the RGC layer.

Visualization of RGCs In Vivo and Comparison of a Fundus Photograph with a Whole Mount Retinal Image

Clear fundus images could be obtained routinely under anesthesia, and mouse RGCs could be identified in vivo at the single-cell level.

By postural change, the superior, inferior, temporal, nasal, and central retina could be visualized. It was difficult, however, to take a photograph of the same living mouse and to achieve acceptable image quality in the peripheral retina, more than 1200 μm from optic disc, or even in the central retina in mice younger than 8 weeks or in those with corneal opacity.

Given that the mice were breathing during ocular fundus photography, a short exposure time was desirable to acquire clearer images without motion blur. However, short exposure time reduces the quality of the images, which was managed by combining three images. Because acute development of lens opacity is frequently encountered under general anesthesia in mice[17] and the pupil diameter of mice is smaller than that of rats, the image quality of mouse fundus photography had been limited. Covering the cornea with mineral oil not only keeps its surface smooth, it prevents the development of lens opacity. The excitation light was concentrated by a 40-D lens to pass small pupils.

To measure the resolution of ocular fundus photography, we compared the fundus photographs (Figs. 3A, 3B) and the images of the whole mount retina (Fig. 3C). This revealed that one pixel in a fundus photograph corresponded to a square of approximately 1.7 × 1.7 μm. The image of RGCs in the fundus photographs showed excellent concordance with that in the whole mount retina (Figs. 3B, 3C).

To verify that longitudinal recording of fundus photographs could be achieved with our methods, we took fundus photographs twice at intervals of 1 week and compared them. Even a single-cell loss could be visualized by our methods (Figs. 3D, 3E).

Reproducibility of Counting the Number of RGCs

To examine reproducibility, we took fundus photographs twice at intervals of 24 hours and counted RGCs manually in the same field of the four square fields, and then we calculated the intraclass correlation (ICC) and the coefficient of variation (CV) between the results obtained from the first and second photographs. The numbers of RGCs in the selected square field (220 × 220 pixels) were 187 ± 21 and 184 ± 22 (mean ± SD; $n = 10$) in the first and second photographs, respectively, the ICC was 0.941, and the CV was 2.1% ± 2.4% (mean ± SD). The density of RGCs in the four areas from nasal, superior, temporal, and inferior quadrants of the central retina were 1505 ± 89/mm^2, 1386 ± 111/mm^2, 1593 ± 139/mm^2, and 1563 ± 68/mm^2, respectively (Table 2). Among each of four areas, no statistical difference in the density of RGCs was seen (Kruskal-Wallis test; $P = 0.054$).

Longitudinal Evaluation of RGCs in Ischemia Reperfusion Models

We recorded fundus photographs longitudinally in the ischemia reperfusion model group and the sham-operated control group to evaluate the longitudinal changes in the number of RGCs in this experimental model. Figures 4A–4J indicate the longitudinal change in the RGC image in one eye after ischemia

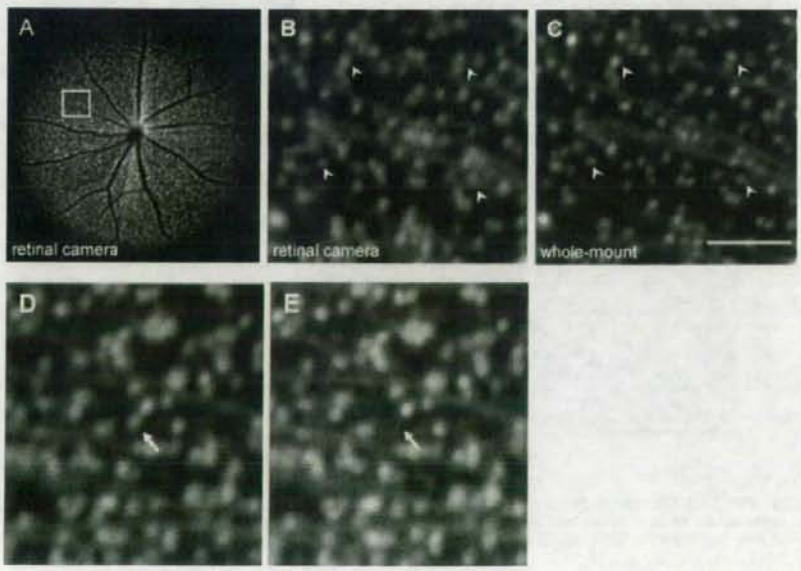

FIGURE 3. (A) Representative examples of mouse ocular fundus photographs. (B, C) Fundus photographs and whole mount of retina corresponding to the *insert* in (A). (B, C, *arrowheads*) Corresponding location. (D, E) RGC loss (*white arrow*) in the control eye could be detected clearly with our method. Scale bar, 100 μm.

TABLE 2. Density of CFP-Expressing RGCs (cells/mm^2) in the Four Areas of the Retina

	Mouse					
Area	1	2	3	4	5	Mean ± SD
Nasal	1525	1637	1511	1401	1449	1505 ± 89
Superior	1285	1381	1527	1271	1462	1386 ± 111
Inferior	1649	1402	1609	1527	1776	1593 ± 139
Temporal	1615	1583	1625	1461	1530	1563 ± 68

reperfusion injury, and Figures 4K and 4L indicate longitudinal change in that the control group.

Reduction of RGC numbers was evaluated sequentially in the same eyes. The number of RGCs and the fluorescence intensity of the nerve fiber decreased considerably during the first week. The percentages of RGCs decreased to 34.2% ± 7.5%, 24.1% ± 9.1%, 23.0% ± 9.3%, and 22.2% ± 8.4% (mean ± SD; $n = 5$) of the percentages before injury at 1, 2, 3, and 4 weeks after the injury, respectively ($P < 0.001$).

The percentages of RGCs in the control eyes were unchanged: 100.5% ± 4.1%, 100.4% ± 3.5%, 101.4% ± 2.3%, and 100.0% ± 3.0% (mean ± SD, $n = 7$) of the percentages before sham operation at 1, 2, 3, and 4 weeks, respectively. The percentages of RGCs with CFP fluorescence after injury to that before injury is shown in Figure 4M.

Histopathologic Evaluation

Figures 5A and 5B show a retinal section of a sham-operated control eye and of that of a treated eye 4 weeks after ischemia reperfusion injury, respectively.

The thickness of the RGC layer and the number of RGCs were markedly reduced in the ischemia reperfusion injury. Moreover, the thickness of the inner plexiform layer was reduced considerably in the ischemia reperfusion injury group

Figures 5C–5E indicate the retrogradely labeled RGCs with DiI in an eye of the ischemia reperfusion injury group in the whole mount retina 4 weeks after injury. In the ischemia reperfusion injury group, DiI$^+$ cells constituted 97.8% ± 3.1% (mean ± SD, five eyes of five mice) and DiI$^-$ cells constituted 2.2% ± 3.1% of the CFP$^+$ cells. Among the DiI$^+$ cells, CFP$^+$ cells constituted

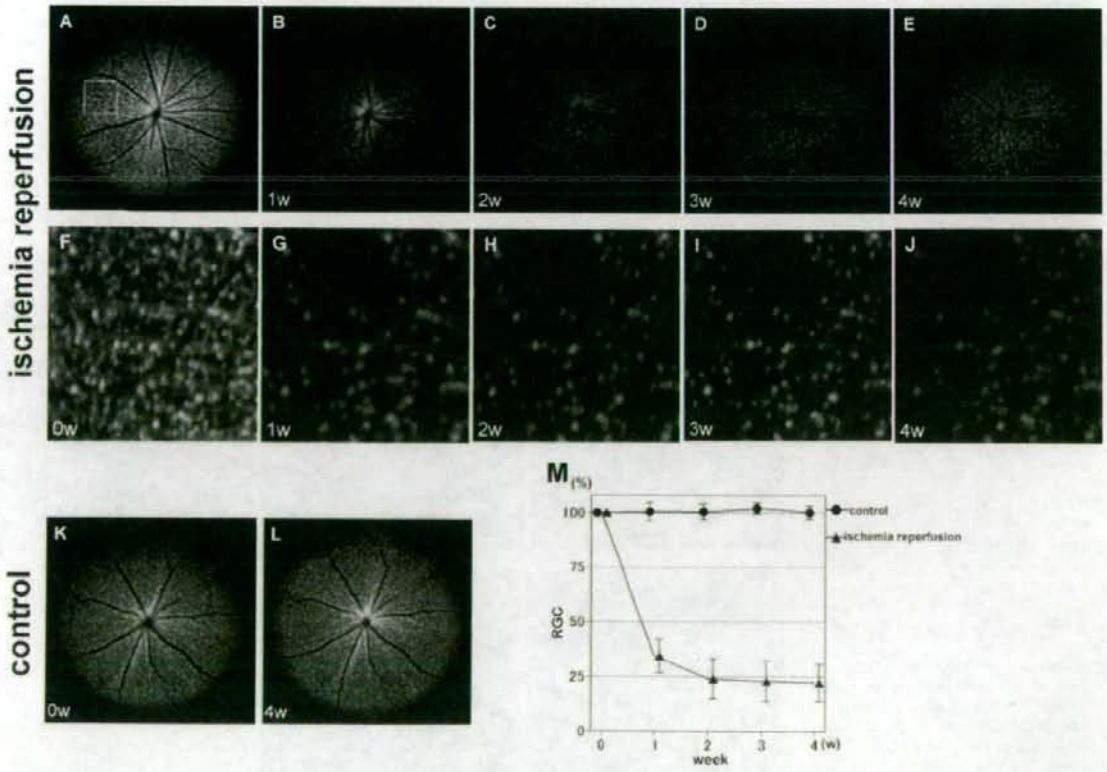

FIGURE 4. Longitudinal evaluation of the ischemia reperfusion injury model group. (**A**, **F**) Presurgery. (**B**, **G**) 1, (**C**, **H**) 2, (**D**, **I**) 3, and (**E**, **J**) 4 weeks after injury. (**F**–**J**) Corresponding area to the *insert* in (**A**). (**K**, **L**) Longitudinal evaluation of the control group. (**M**) Longitudinal changes of RGCs. The survival ratio of RGCs in postoperative period against that in the preoperative period in the control group ($n = 7$, *circles*) and the ischemia reperfusion injury model group ($n = 5$, *triangles*). Error bars indicate SD.

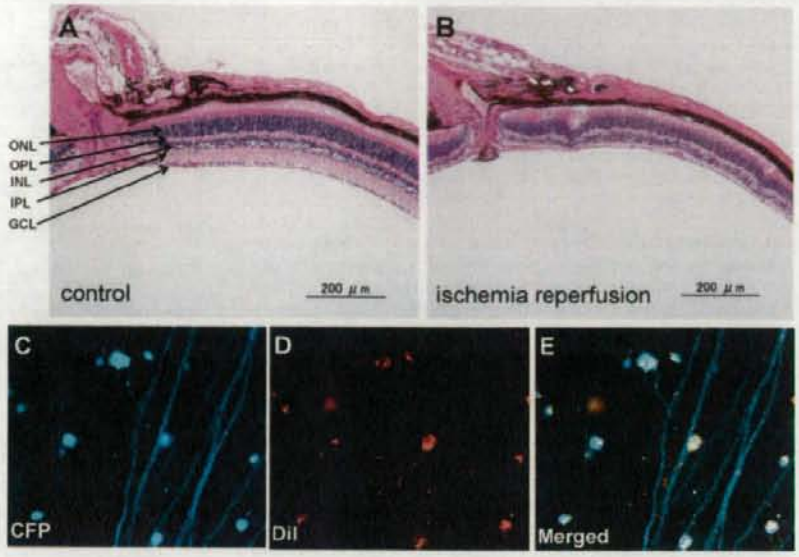

FIGURE 5. (**A**, **B**) Histologic evaluation of paraffin-embedded, hematoxylin/eosin-stained retinal sections. (**A**) Four weeks after sham operation and (**B**) 4 weeks after ischemia reperfusion injury. GCL, ganglion cell layer; IPL, inner plexiform layer; INL, inner nuclear layer; OPL, outer plexiform layer; ONL, outer nuclear layer. (**C**–**E**) Whole mount retina 4 weeks after ischemia reperfusion injury. Scale bars, 100 μm.

59.2% ± 3.4% and CFP^- cells constituted 40.8% ± 3.4% (Figs. 5C–E; Table 1). The percentage of the CFP^+ cells among the DiI^+ cells in the ischemia reperfusion injury group was significantly less than that in the control group ($P = 0.03$ by unpaired *t*-test; 59.2% ± 3.4% vs. 72.6% ± 5.2%).

DISCUSSION

Experimental mouse models are often applied to investigate the pathophysiology of human diseases. In vivo observation of apoptotic RGCs labeled with intravitreously injected Annexin V[18] and of retrogradely labeled RGCs after injection of a fluorescent dye into the superior colliculus[19] were reported in a rat model. Annexin V can bind to externalized phosphatidylserine, reflecting a preapoptotic condition,[18] but intravitreous injection may limit the experimental protocols and affect outcomes. Moreover, longitudinal counting of apoptotic RGCs was not performed in that study.[18] Fluorochromes such as DiA, DiI, and 4Di-10-ASP have often been used for labeling RGCs, but injection of exogenous dye into the superior colliculus is required, and sometimes RGCs are not labeled uniformly. Frequently used neurotracers are relatively stable, and microglia can be labeled secondarily by phagocytosing degenerated RGCs.[19,20] Lastly, genetic modification and experimental tools are less available in the rat than in the mouse.

Feng et al.[8] recently developed transgenic mice expressing CFP in living RGCs, which allowed us to visualize RGCs histologically. This mouse also paves the way for noninvasive observation of living RGCs in vivo. One of the benefits of the transgenic mouse is that it enables more precise cell counting than does the mouse with retrogradely labeled RGCs because CFP expression in the cytosol could delineate the cell body of RGCs whereas DiI is detected as particles in the RGC cytosol. Thus, some overlaid or adjacent cells were distinguished easily by the margin of CFP-stained cytosol (Figs. 2A–2C). Although our method relied on manual counting of CFP-stained RGCs as previous retrograde labeling method,[19] reproducibility of the result given by a masked, experienced investigator was thought to be sufficiently high.

In our devices, a pixel in the fundus photograph corresponds to approximately 1.7 × 1.7 μm, and an RGC soma measures 5 μm or more.[21] Thus, theoretically our system has sufficient resolution to detect an individual RGC. Comparison of ocular fundus images and the whole mount retina of the same eye confirmed that our method could capture almost all RGCs expressing CFP (Figs. 3B, 3C), and even the loss of a single cell could be detected with our method (Figs. 3D, 3E).

Available methods to evaluate experimental neurodegeneration by counting RGCs in the whole mount retina[22] or by measuring the thickness of retinal sections[12] require a large number of experimental animals and are limited in their ability to detect subtle changes in RGCs. We could detect RGC reduction with a smaller number of mice without sacrificing them by in vivo sequential imaging of the same region in a single eye.

Ocular fundus images of mice have been obtained in two ways: by means of a retinal camera[23] (a conventional method of fundus photography) and by cSLO.[14–16,24,25] In cSLO, the obtained image measures only 768 × 768 pixels,[26] and the detectable fluorescence is limited because of the limitation of available wavelength for excitation light (460 nm, 488 nm, 514 nm, 795 nm, and 830 nm).[14,25] Although these reports do not clearly mention the actual image area taken by one shot, montage photographs or several shots are required to evaluate a sufficiently wide area of the retina. On the other hand, approximately 25% of the whole RGCs (1700 × 1700 μm) can be longitudinally photographed in the same area of the same retina as one image by our method with a retinal camera. Moreover, a retinal camera, which is more cost-effective than cSLO, can support the use of various fluorescent dyes by changing fluorescence filters. One of the limitations is that RGCs in the peripheral retina 1200 μm or more apart from the disc could not be evaluated by our method because of the difficulty of taking images of acceptable quality. Thus, approximately central 36% of the whole area of the retina can be evaluated by the current method. This limitation that the whole retina could not be evaluated by our in vivo fundus photography also applied to the methods of in vivo imaging with Annexin V staining[18] or of scanning laser ophthalmoscopy.[19] In addition, it is challenging to take retinal photographs of mouse eyes younger than 8 weeks of age or with corneal opacity.

B6.Cg-Tg(Thy1-CFP)23Jrs/J mice express CFP in some amacrine cells, and all RGCs do not always express CFP.[8] Thus, with our method, some amacrine cells may be co-counted as a total number, but some RGCs may not be counted. However, CFP^+ and DiI^- cells, which are considered to be CFP^+ amacrine cells, were only 3% of the total CFP^+ cells, and CFP^+ and DiI^+ cells, which are considered to be CFP^+ RGCs, were approximately 73% of the total DiI^+ cells. Thus, any amacrine cells included should have only a minor effect on the RGC count.

One intriguing finding is that the percentage of CFP^+ cells among the DiI^+ cells in ischemia-reperfusion group 4 weeks after injury was significantly lower than that in the untreated group (59.2% vs. 72.6%). It was reported previously that $Thy1^+$ RGCs decrease rapidly after injury,[27,28] and Thy1 is a more sensitive marker of injured RGCs.[29] In our system, CFP^+ cells are thought to reflect $Thy1^+$ cells indirectly because the expression of CFP and Thy1 is linked genetically in this transgenic mouse. Thus, CFP^- RGCs after injury may reflect dysfunction of a basic cellular activity, gene transcription. On the other hand, DiI or other imported particles do not reflect cellular activity, even though they are observed in the cell body, because they can remain in the cells as long as the cell structure is conserved. In fact, our study indicated that injured RGCs after ischemia reperfusion detected by CFP fluorescent fadeaway progressed earlier than they did in other studies.[13] Thus, our system using CFP expression linked with Thy1 to detect cell injury may have advantages in the sensitivity to detect the earlier changes of cell death compared with other labeling methods.

In vivo imaging in neurodegenerative mouse models has many advantages.[30] By using our method to evaluate the number of RGCs longitudinally in the same animals, it is possible to monitor the time course of RGC injury or neuroprotective effects of drugs. Moreover, cross-breeding of various genetically modified mice and CFP-expressing mice would have great potential in investigating the time course of RGC death. Our technique may open up the possibility of detailed investigations of neurodegeneration or nerve regeneration through mouse eyes.

Acknowledgments

The authors thank Aya Iriyama and Masaaki Ohashi for histologic evaluation.

References

1. Burgoyne CF. Image analysis of optic nerve disease. *Eye.* 2004;18:1207–1213.
2. Fujimoto JG. Optical coherence tomography for ultrahigh resolution in vivo imaging. *Nat Biotechnol.* 2003;21:1361–1367.
3. Quigley HA. Number of people with glaucoma worldwide. *Br J Ophthalmol.* 1996;80:389–393.
4. Clark AF, Yorio T. Ophthalmic drug discovery. *Nat Rev Drug Discov.* 2003;2:448–459.
5. Goldberg I. Relationship between intraocular pressure and preservation of visual field in glaucoma. *Surv Ophthalmol.* 2003;48(suppl 1):S3–S7.
6. Fechtner RD, Weinreb RN. Mechanisms of optic nerve damage in primary open angle glaucoma. *Surv Ophthalmol.* 1994;39:23–42.
7. Goldblum D, Mittag T. Prospects for relevant glaucoma models with retinal ganglion cell damage in the rodent eye. *Vision Res.* 2002;42:471–478.
8. Feng G, Mellor RH, Bernstein M, et al. Imaging neuronal subsets in transgenic mice expressing multiple spectral variants of GFP. *Neuron.* 2000;28:41–51.
9. Shaner NC, Steinbach PA, Tsien RY. A guide to choosing fluorescent proteins. *Nat Methods.* 2005;2:905–909.
10. Harada C, Harada T, Slusher BS, Yoshida K, Matsuda H, Wada K. N-acetylated-alpha-linked-acidic dipeptidase inhibitor has a neuroprotective effect on mouse retinal ganglion cells after pressure-induced ischemia. *Neurosci Lett.* 2000;292:134–136.
11. Aihara M, Lindsey JD, Weinreb RN. Reduction of intraocular pressure in mouse eyes treated with latanoprost. *Invest Ophthalmol Vis Sci.* 2002;43:146–150.
12. Lam TT, Abler AS, Tso MO. Apoptosis and caspases after ischemia-reperfusion injury in rat retina. *Invest Ophthalmol Vis Sci.* 1999;40:967–975.
13. Lafuente MP, Villegas-Perez MP, Selles-Navarro I, et al. Retinal ganglion cell death after acute retinal ischemia is an ongoing process whose severity and duration depends on the duration of the insult. *Neuroscience.* 2002;109:157–168.
14. Seeliger MW, Beck SC, Pereyra-Munoz N, et al. In vivo confocal imaging of the retina in animal models using scanning laser ophthalmoscopy. *Vision Res.* 2005;45:3512–3519.
15. Luhmann UF, Lin J, Acar N, et al. Role of the Norrie disease pseudoglioma gene in sprouting angiogenesis during development of the retinal vasculature. *Invest Ophthalmol Vis Sci.* 2005;46:3372–3382.
16. Paques M, Simonutti M, Roux MJ, et al. High resolution fundus imaging by confocal scanning laser ophthalmoscopy in the mouse. *Vision Res.* 2006;46:1336–1345.
17. Calderone L, Grimes P, Shalev M. Acute reversible cataract induced by xylazine and by ketamine-xylazine anesthesia in rats and mice. *Exp Eye Res.* 1986;42:331–337.
18. Cordeiro MF, Guo L, Luong V, et al. Real-time imaging of single nerve cell apoptosis in retinal neurodegeneration. *Proc Natl Acad Sci U S A.* 2004;101:13352–13356.
19. Higashide T, Kawaguchi I, Ohkubo S, Takeda H, Sugiyama K. In vivo imaging and counting of rat retinal ganglion cells using a scanning laser ophthalmoscope. *Invest Ophthalmol Vis Sci.* 2006;47:2943–2950.
20. Thanos S, Kacza J, Seeger J, Mey J. Old dyes for new scopes: the phagocytosis-dependent long-term fluorescence labelling of microglial cells in vivo. *Trends Neurosci.* 1994;17:177–182.
21. Perry VH. Evidence for an amacrine cell system in the ganglion cell layer of the rat retina. *Neuroscience.* 1981;6:931–944.
22. Inoue T, Hosokawa M, Morigiwa K, Ohashi Y, Fukuda Y. Bcl-2 overexpression does not enhance in vivo axonal regeneration of retinal ganglion cells after peripheral nerve transplantation in adult mice. *J Neurosci.* 2002;22:4468–4477.
23. Hawes NL, Smith RS, Chang B, Davisson M, Heckenlively JR, John SW. Mouse fundus photography and angiography: a catalogue of normal and mutant phenotypes. *Mol Vis.* 1999;5:22.
24. Jaissle GB, May CA, Reinhard J, et al. Evaluation of the rhodopsin knockout mouse as a model of pure cone function. *Invest Ophthalmol Vis Sci.* 2001;42:506–513.
25. Leung CK, Lindsey JD, Crowston JG, et al. In vivo imaging of murine retinal ganglion cells. *J Neurosci Methods.* 2008;168:475–478.
26. Jorzik JJ, Bindewald A, Dithmar S, Holz FG. Digital simultaneous fluorescein and indocyanine green angiography, autofluorescence, and red-free imaging with a solid-state laser-based confocal scanning laser ophthalmoscope. *Retina.* 2005;25:405–416.
27. Schlamp CL, Johnson EC, Li Y, Morrison JC, Nickells RW. Changes in Thy1 gene expression associated with damaged retinal ganglion cells. *Mol Vis.* 2001;7:192–201.
28. Huang W, Fileta J, Guo Y, Grosskreutz CL. Downregulation of Thy1 in retinal ganglion cells in experimental glaucoma. *Curr Eye Res.* 2006;31:265–271.
29. Chidlow G, Casson R, Sobrado-Calvo P, Vidal-Sanz M, Osborne NN. Measurement of retinal injury in the rat after optic nerve transection: an RT-PCR study. *Mol Vis.* 2005;11:387–396.
30. Misgeld T, Kerschensteiner M. In vivo imaging of the diseased nervous system. *Nat Rev Neurosci.* 2006;7:449–463.

Laser Scanning Tomography of Optic Discs of the Normal Japanese Population in a Population-based Setting

Haruki Abe, MD, PhD,[1] Motohiro Shirakashi, MD, PhD,[1] Tae Tsutsumi, MD,[2,3] Makoto Araie, MD, PhD,[3] Atsuo Tomidokoro, MD, PhD,[3] Aiko Iwase, MD, PhD,[2] Goji Tomita, MD, PhD,[4] Tetsuya Yamamoto, MD, PhD,[5] Tajimi Study Group

Objective: To evaluate the optic disc characteristics using the Heidelberg retina tomograph (HRT) II in a large sample of normal Japanese subjects.

Design: Cross-sectional study.

Participants: A total of 3576 eyes of 2036 normal subjects, with good-quality HRT II images, of 6042 eyes of 3021 subjects aged 40 years or more who participated in the Tajimi Study, a population-based eye study in Japan.

Methods: Optic disc parameters were obtained using HRT II, and the association of gender, age, height, weight, blood pressure, ocular perfusion pressure, refraction, intraocular pressure (IOP), central corneal thickness (CCT), and disc size on HRT parameters was assessed using simple and multiple regression analyses.

Main Outcome Measures: HRT parameters, including disc area, cup area, rim area, cup-to-disc area ratio, cup volume, rim volume, mean cup depth, maximum cup depth, height variation contour, cup shape measure, mean retinal nerve fiber layer (RNFL) thickness, and RNFL cross-sectional area, and the crude and partial correlations of the potential confounders with the HRT parameters.

Results: Disc area, cup-to-disc area ratio, and rim area averaged 2.06 ± 0.41 mm^2 (mean±standard deviation), 0.23 ± 0.13, and 1.55 ± 0.29 mm^2, respectively. All HRT parameters were strongly or moderately correlated between right and left eyes (Pearson's correlation coefficients = 0.45–0.83, $P<0.001$). Absolute inter-eye differences in several HRT parameters were positively correlated with disc area ($P<0.05$). Multiple regression analyses adjusting for the confounders showed weak but significant correlations of height, refractive error, IOP, and CCT with several HRT parameters (partial correlation coefficient (absolute value) = 0.04–0.16, $P<0.05$), and moderate or weak but significant correlations of disc area with all HRT parameters (partial correlation coefficient [absolute value] = 0.05–0.73, $P<0.05$). Gender, weight, blood pressure, and ocular perfusion pressure did not significantly correlate with HRT parameters.

Conclusions: This report presents reference data of normality for the HRT parameters based on a large sample of normal Japanese subjects. There were small but significant influences of height, refractive error, IOP, and CCT on several HRT parameters. Many HRT parameters were moderately or weakly affected by disc size.

Financial Disclosure(s): Proprietary or commercial disclosure may be found after the references.
Ophthalmology 2009;116:223–230 © 2009 by the American Academy of Ophthalmology.

Because structural changes of the optic disc often precede the development of visual field loss in glaucoma,[1–5] detection of optic disc damage plays a vital role in the diagnosis of glaucoma, especially in its early stages. Although ophthalmoscopy and fundus photography are still widely used for assessing glaucomatous optic disc damage, they are limited by their subjective and qualitative nature.[6–8] With the development of optic nerve imaging instruments, objective and quantitative measurements of the optic disc have become available. A confocal scanning laser ophthalmoscope, such as the Heidelberg retina tomograph (HRT) or HRT II (Heidelberg Engineering, Heidelberg, Germany), allows 3-dimensional topographic analysis of the optic disc and provides a quantitative measure of a variety of optic disc parameters.[9–12]

Understanding of normal optic disc shape and related factors are of critical importance in improving the performance of confocal scanning laser ophthalmoscope to determine glaucomatous changes in the optic disc. Distributions or ranges of the optic disc parameters determined with confocal scanning laser ophthalmoscope in large samples of normal subjects (number of subjects >~500) have been reported by Hermann et al.[13] (1764 eyes of 882 subjects) and Vernon et al.[14] (918 eyes of 459 subjects) in white populations. Because there are racial differences in optic disc characteristics,[15–19] it is worthwhile accumulating such

ISSN 0161-6420/09/$–see front matter
doi:10.1016/j.ophtha.2008.09.013

information for each of the various ethnicities. For Asian populations, however, to our knowledge, there are only the Turkish hospital-based study by Durukan et al.[20] (1102 eyes of 551 subjects) and 2 Japanese hospital-based studies with relatively small sample sizes by Nakamura et al.[21] (77 eyes of 77 subjects) and Uchida et al.[22] (223 eyes of 223 subjects).

We recently conducted the Tajimi Study, a population-based eye study focusing primarily on estimating the prevalence of glaucoma among Japanese persons aged 40 years or more.[23–27] The purposes of the present report were to evaluate the optic disc characteristics by means of HRT II in a large sample of ophthalmologically normal Japanese subjects who participated in the Tajimi Study and to evaluate associations of possibly related systemic and ocular factors, including gender, age, height, weight, blood pressure, ocular perfusion pressure (OPP), refractive error, intraocular pressure (IOP), central corneal thickness (CCT), and optic disc size with the optic disc characteristics.

Subjects and Methods

Population Sampling

The Tajimi Study, a population-based eye study of Japanese subjects aged 40 years or more was conducted between September of 2000 and October of 2001 in Tajimi City, Japan.[23–27] The details of the Tajimi Study have been published.[23–27] Briefly, of 54,165 inhabitants aged 40 years or more in Tajimi City as of August 1, 2000, 4000 were selected randomly without stratification and were encouraged to participate in the epidemiologic study. The investigation followed the tenets of the World Medical Association's Declaration of Helsinki and the municipal statutes of Tajimi City for protecting personal information; the study protocol was approved by the ethics committee of Tajimi City. Written informed consent was obtained from all participants after the details of the study had been explained fully. Among the selected 4000 participants, 48 died and 82 were not actual residents of or had moved from Tajimi City during the screening period. Of the remaining 3870 persons, 3021 participated in the screening examinations.

Ocular Examinations

Screening and definitive examinations have been reported in detail.[23–27] Briefly, the screening examinations included not only ocular parameters but also parameters such as height, weight, and blood pressure. OPP was calculated as "2/3[diastolic blood pressure + 1/3(systolic blood pressure—diastolic blood pressure)]–IOP." The ocular examinations included measurement of refractive status and corneal curvature using an autorefractometer (KP-8100PA, Topcon, Tokyo, Japan), visual acuity using a Landolt ring chart at a distance of 5 m with refractive correction, and CCT using a specular-type pachymeter (SP-2000P, Topcon), slit-lamp biomicroscopic examination, evaluation of angle width according to the van Herick method, IOP measurement by Goldmann applanation tonometry, fundus examination based on digital color photographs obtained through an undilated pupil using the IMAGEnet digital fundus camera system (TRC-NW6S, Topcon) with angles of 30 and 45 degrees, visual field screening using a frequency doubling technology screener (Humphrey Instruments, San Leandro, CA) with the C-20–1 screening test, and optic disc measurements using HRT II (software version 1.4.1). Participants were referred for definitive examination if ocular disorders or related conditions were suspected and if they met 1 or more of the following criteria: corrected visual acuity <20/30; abnormal findings on slit-lamp examination or on fundus photographs; IOP >19 mmHg (i.e., mean + 2 × standard deviation of the IOP values previously reported in ~12,000 Japanese eyes[28]); angle width grade 2 or less (van Herick method); findings in the optic disc, retina, or both suggestive of glaucoma or other ocular diseases; and at least 1 abnormal test point in the frequency doubling technology visual field test. The definitive examination included slit-lamp examination, gonioscopy, optic disc and posterior pole fundus evaluation with a Goldmann 2-mirror lens (Haag-Streit, Koeniz, Switzerland), applanation tonometry, and visual field testing with the Humphrey Perimeter Central 30–2 Swedish Interactive Threshold Algorithm Standard program (Humphrey Instruments). Unless gonioscopy revealed an occludable angle, the pupil was dilated to obtain stereoscopic disc photographs (3-DX NM; Nidek, Gamagori, Japan) and to observe the ocular fundus in detail by indirect ophthalmoscopy. When the angle was thought to be occludable, the same examinations were carried out with undilated pupils.

Optic Disc Measurements using HRT II

In the screening examination, optic disc parameters were measured using HRT II. HRT II uses a diode laser (670-nm wavelength) to sequentially scan the retinal surface in the horizontal and vertical directions at multiple focal planes. By using confocal scanning principles, a 3-dimensional topographic image is constructed from a series of optical image sections at consecutive focal planes. The topographic image determined from the acquired 3-dimensional image consists of 384×384 (147,456) pixels, each of which is a measurement of retinal height at its corresponding location. For every subject in this study, images were obtained through undilated pupils with a 15-degree field of view. Three topographic images were obtained, combined, and automatically aligned to make a single mean topographic image for analysis. A contour line of the optic disc margin was drawn around the inner margin of the peripapillary scleral ring by one experienced examiner (TT), who was masked to the other clinical information, with viewing nonstereo color fundus photographs. The contour line was reviewed in the topography and reflectance images and the height profile graph included in the instrument by the same examiner. For approximately 500 HRT images randomly chosen, another experienced examiner (GT) double-checked the contour lines and confirmed the correctness of the placement. Twelve HRT parameters obtained with routine analysis were analyzed: disc area, cup area, rim area, cup-to-disc area ratio, cup volume, rim volume, mean cup depth, maximum cup depth, height variation contour, cup shape measure, mean retinal nerve fiber layer (RNFL) thick-

ness, and RNFL cross-sectional area. Magnification errors were corrected using subjects' refractive status and corneal curvature measurements. This instrument and these parameters have been described.[14,17,20,29]

Data Analysis

In the present study, the analysis was restricted to eyes that had valid optic disc measurements with HRT II. Good image quality was defined by appropriate focus, brightness and clarity, minimal eye movement, optic disc centered in the image, and a standard deviation of the mean topographic image <40 μm. Eyes in which good-quality images could not be obtained were excluded from the analysis. Eyes of normal subjects based on the screening and definitive examinations were included in the analysis. Normal subjects had a best corrected visual acuity ≥20/30, spherical refraction ≤±5 diopters (D), cylinder correction ≤±3 D, a normal IOP ≤21 mmHg, normal appearance of the optic disc and ocular fundus, normal visual field by frequency doubling technology screener or Humphrey perimeter, no previous laser surgery or intraocular surgery, and no significant ocular disease. Patients with glaucoma, suspected glaucoma, IOP >21 mmHg, or exfoliation in at least 1 eye or those with eyes having any inborn aberrations (e.g., tilted disc) were carefully excluded.

Data were analyzed using SPSS 14.0J for Windows (SPSS Japan, Inc., Tokyo, Japan). Comparisons between groups were analyzed with paired or unpaired t test or the chi-square test. Pearson's correlation coefficients were calculated to assess correlations between the 2 variables. Multiple regression analysis was applied to adjust for the effects of potential confounders. All tests were 2-tailed. Because the sample size in the current report was sufficiently large (i.e., >1700 right and 1800 left eyes), parametric tests, including t test, Pearson's correlation coefficient, and multiple regression, were used based on the central limit theorem.

Results

Of 6042 eyes of the 3021 participants of the Tajimi Study, reliable HRT II results in ophthalmologically normal eyes were analyzed in 3576 eyes (1769 right eyes and 1807 left eyes) of 2036 participants. Between the included and excluded subjects, the male/female ratio was not statistically different (924/1112 vs. 410/575, $P = 0.051$, χ^2 test), whereas age was significantly younger in the included subjects than in the excluded subjects (56.0±10.0 years vs. 63.4±13.7 years, $P<0.001$, unpaired t test). The reasons for exclusion were (1) subjects were screened in their own home (88 eyes); (2) HRT II measurements could not be completed at the screening sites for various reasons, such as subjects' ocular or physical problems (906 eyes); and (3) standard deviation of the HRT II measurements was ≥40 μm (640 eyes). Eyes of definitive glaucoma, suspected glaucoma, pseudoexfoliation, primary angle closure, ocular hypertension or fellow eyes of these eyes (364 eyes), eyes with other ocular diseases including congenital disc anomalies that could affect the disc shape (84 eyes), pseudophakic eyes (41 eyes), eyes with excessive refractive errors (spherical error >±5 D or cylindrical error >±3 D) (260 eyes), and eyes with best corrected visual acuity worse than 20/30 (83 eyes) were also excluded.

Inter-eye Difference in HRT Parameters

HRT parameters were compared between right and left eyes in 1540 normal subjects, of whom both eyes were eligible. All HRT parameters were significantly correlated between right and left eyes (Pearson's correlation coefficients ≥0.450, $P<0.001$) (Table 1 [available at http://aaojournal.org]). Rim volume and height variation contour showed small but significant inter-eye difference ($P<0.001$, paired t test), whereas the other parameters did not. The absolute differences in HRT parameters between right and left eyes are also shown in Table 1 (available at http://aaojournal.org). Among HRT parameters, inter-eye absolute difference was significantly different between male and female subjects only in cup shape measure (0.05±0.04 and 0.06±0.05, respectively, $P = 0.001$), and the difference was still significant ($P = 0.027$) in multiple regression analyses adjusting for age, height, weight, systolic and diastolic blood pressure, OPP, refractive error, IOP, and CCT. Multiple regression analyses adjusting for these confounders and gender showed that disc area (mean value of right and left eyes) was significantly positively correlated with inter-eye absolute difference in cup area, rim area, cup volume, rim volume, and RNFL cross-sectional area ($P<0.05$), suggesting subjects having larger discs tended to show greater inter-eye absolute differences in these HRT parameters, whereas disc area was significantly negatively correlated with the inter-eye absolute difference in cup shape measure ($P<0.001$). Because all HRT parameters were significantly correlated and the results of the analyses were similar between right and left eyes, only the results from the right 1769 eyes (787 male and 982 female subjects) are presented in the following sections.

Association of Gender, Age, Height, Weight, and Blood Pressure with HRT Parameters

A total of 787 male subjects had significantly older age, heavier weight, taller height, higher systolic and diastolic blood pressure, and higher OPP and thicker CCT than 982 female subjects (unpaired t test, $P\leq0.009$), whereas refractive error and IOP were not significantly different ($P\geq0.126$) (Table 2).

In simple regression analyses, age was negatively correlated with disc area, rim area, rim volume, maximum cup depth, height variation contour, mean RNFL thickness, and RNFL cross-sectional area in both male and female subjects ($P\leq0.002$) (Table 3 [available at http://aaojournal.org]). These trends are also seen after adjusting for the potential confounders using multiple regression analysis (Tables 4 and 5 [available at http://aaojournal.org]). Cup area and cup-to-disc area ratio were significantly greater in male subjects than female subjects ($P\leq0.004$). However, after adjusting for the potential confounders, gender-related dif-

Table 2. Comparison of Demographic Data and Heidelberg Retina Tomograph Parameters of Normal Right Eyes between 787 Male and 982 Female Subjects

	All	Male	Female	P*
Age (y)	55.7±9.8 (55.3–56.2)	56.4±9.8 (55.7–57.1)	55.2±9.9 (54.5–55.8)	0.009
Weight (kg)	58.2±10.6 (57.7–58.7)	63.9±10.1 (63.2–64.6)	53.7±8.9 (53.1–54.3)	<0.001
Height (cm)	158.9±8.8 (158.5–159.3)	165.6±6.7 (165.7–166.1)	153.3±6.3 (152.9–153.8)	<0.001
Systolic blood pressure (mmHg)	130.4±22.7 (129.3–131.4)	133.5±22.3 (131.9–135.1)	128.9±22.8 (127.3–130.5)	<0.001
Diastolic blood pressure (mmHg)	78.8±13.2 (78.1–79.4)	80.9±13.2 (80.0–81.8)	77.2±13.1 (76.3–78.2)	<0.001
OPP (mmHg)	49.5±9.8 (49.1–50.0)	51.1±9.6 (50.4–51.7)	48.5±9.8 (47.8,49.2)	<0.001
Refractive error (diopters)†	−0.4±1.7 (−0.5 to −0.4)	−0.5±1.8 (−0.6 to −0.3)	−0.4±1.8 (−0.6 to −0.3)	0.612
IOP (mmHg)	14.4±2.5 (14.3–14.6)	14.6±2.6 (14.4–14.8)	14.5±2.4 (14.3–14.6)	0.126
CCT (μm)	520±32 (518–521)	525±33 (523–527)	516±31 (514–518)	<0.001
Disc area (mm^2)‡	2.06±0.41 (2.04–2.08)	2.08±0.44 (2.04–2.11)	2.05±0.39 (2.02–2.08)	0.085
Cup area (mm^2)‡	0.51±0.35 (0.49–0.53)	0.54±0.37 (0.51–0.56)	0.50±0.32 (0.47–0.52)	0.002
Rim area (mm^2)‡	1.55±0.29 (1.54–1.56)	1.54±0.29 (1.52–1.56)	1.55±0.29 (1.53–1.57)	0.181
Cup-to-disc area ratio‡	0.23±0.13 (0.23–0.24)	0.24±0.13 (0.23–0.25)	0.23±0.12 (0.22–0.24)	0.004
Cup volume (mm^3)‡	0.11±0.12 (0.11–0.12)	0.12±0.12 (0.11–0.13)	0.11±0.11 (0.10–0.12)	0.006
Rim volume (mm^3)‡	0.41±0.14 (0.40–0.42)	0.40±0.14 (0.39–0.41)	0.42±0.14 (0.41–0.43)	0.083
Mean cup depth (mm)‡	0.21±0.09 (0.20–0.21)	0.21±0.09 (0.20–0.22)	0.20±0.09 (0.20–0.21)	0.034
Maximum cup depth (mm)‡	0.57±0.20 (0.56–0.58)	0.58±0.20 (0.56–0.59)	0.57±0.21 (0.56–0.59)	0.157
Height variation contour (mm)‡	0.38±0.09 (0.38–0.39)	0.38±0.10 (0.38–0.39)	0.39±0.10 (0.38–0.39)	0.572
Cup shape measure‡	−0.19±0.07 (−0.19 to −0.19)	−0.19±0.07 (−0.19 to −0.18)	−0.19±0.07 (−0.20 to −0.19)	0.033
Mean RNFL thickness (mm)‡	0.25±0.07 (0.25–0.26)	0.25±0.07 (0.25–0.25)	0.26±0.07 (0.25–0.26)	0.007
RNFL cross-sectional area (mm^2)‡	1.29±0.35 (1.27–1.30)	1.27±0.35 (1.24–1.29)	1.31±0.35 (1.28–1.33)	0.028

RNFL = retinal nerve fiber layer; OPP = ocular perfusion pressure; IOP = intraocular pressure; CCT = central corneal thickness.
Data are shown as "mean±standard deviation (95% confidence interval)."
*P value on comparison between male and female subjects (unpaired t test).
†Spherical equivalent values.
‡Because of multiple comparisons among the 12 Heidelberg Retina Tomograph parameters, Bonferroni correction was applied with a level of significance of 0.0042.

ference in HRT parameters did not reach statistical significance ($P>0.05$) (Tables 4 and 5 [available at http://aaojournal.org]). Height was also weakly correlated with several HRT parameters in simple and multiple regression analyses (Tables 3, 4, and 5 [available at http://aaojournal.org]). Although disc area was not significantly correlated with height in multiple regression analysis, cup-related parameters were positively correlated with height, whereas rim-related parameters were negatively correlated with height (Tables 4 and 5 [available at http://aaojournal.org]). Weight was not correlated significantly with any HRT parameters in multiple regression analyses (Tables 4 and 5 [available at http://aaojournal.org]). Systolic blood pressure and OPP were negatively correlated with some HRT parameters in simple regression analyses, but the significant correlations disappeared after adjusting for the potential confounders (Tables 3, 4, and 5 [available at http://aaojournal.org]).

Association of Refractive Error, IOP, and CCT with HRT Parameters

Multiple regression analysis showed weak but significant positive correlation between refractive error and disc area ($P<0.001$), suggesting the trend that more myopic eyes had smaller discs (Table 4 [available at http://aaojournal.org]). Rim volume, mean RNFL thickness, and RNFL cross-sectional area were negatively correlated with refractive error in both male and female subjects in simple regression analyses ($P<0.001$) and multiple regression analyses ($P<0.001$) (Tables 3 and 4 [available at http://aaojournal.org]), suggesting that more myopic eyes had greater rim volume. Rim volume, mean RNFL thickness, and RNFL cross-sectional area were still negatively correlated with refractive error after adjusting for disc area and the other potential confounders (Table 5 [available at http://aaojournal.org]).

IOP was positively correlated with some cup-related parameters in multiple regression analyses ($P<0.05$) (Table 5 [available at http://aaojournal.org]), suggesting the trend that eyes with higher IOP had greater cup. CCT showed weak but significant negative correlations with cup volume in multiple regression analyses ($P<0.05$) (Tables 4 and 5 [available at http://aaojournal.org]).

Association of Disc Area with the Other HRT Parameters

Disc area was correlated with all HRT parameters except height variation contour with P values of ≤0.001 (Table 6 [available at http://aaojournal.org]). Cup area and cup volume were relatively strongly correlated with disc area (Pearson's correlation coefficients ≥0.61). In multiple regression analyses after adjusting for the potential confounders, disc area was also correlated with all HRT parameters except height variation contour with P values <0.001 (Table 5).

Discussion

A total of 3576 eyes of 2036 ophthalmologically normal Japanese subjects who participated in the Tajimi Study[23–27] were included in the present analyses. The age distribution of the Tajimi Study participants was similar to that of the Japanese population.[23,30] In the Tajimi Study, although the distribution of IOP was widely overlapped between normal and glaucoma eyes,[23] the criteria for diagnosing glaucoma were not based on IOP, but on findings in the visual field and optic disc in accordance with the criteria of the International Society for Geographical and Epidemiological Ophthalmology.[31] Moreover, ophthalmologically normal eyes in the current analyses were selected according to more strict criteria as described previously. Thus, these criteria should achieve reasonably high specificity of normal eyes in the present report.

In the present report, descriptive statistics of the HRT parameters in the population were presented. All HRT parameters were strongly or moderately correlated between right and left eyes. Absolute inter-eye differences in several HRT parameters were positively correlated with disc area. Multiple regression analyses adjusting for the potential confounders showed weak but significant correlations of height, refractive error, IOP, and CCT with several HRT parameters, and moderate or weak but significant correlations of disc area with many HRT parameters. Gender, weight, blood pressure, and OPP did not significantly correlate with HRT parameters.

Several investigators have reported racial differences in optic disc characteristics.[15–19] In normal subjects of various races, Tsai et al.,[15] using HRT, found that disc area, cup area, cup-to-disc area ratio, cup volume, and maximum cup depth were significantly greater in 43 African-Americans than in 44 whites, with intermediate values for 45 Asians and 48 Hispanics. In another study of normal subjects, Girkin et al.,[17] using HRT II, found significantly greater disc area, cup area, rim area, cup volume, mean cup depth, and mean RNFL thickness in 144 normal eyes (84 subjects) of African-Americans than in 109 normal eyes of 68 white subjects. In normal white subjects, Hermann et al.,[13] using HRT, reported that the mean disc area was 1.82 mm^2 (882 subjects), and Vernon et al.[14] (459 subjects), using HRT II, reported that the mean and median disc areas were 1.98 and 1.93 mm^2, respectively. Girkin et al.,[17] using HRT II, reported that the mean disc areas were 2.26 mm^2 for normal African-American subjects and 1.98 mm^2 for normal white subjects. In the present report on 2036 normal Japanese subjects using HRT II, the mean disc area was 2.06 mm^2 (Table 2). The normal range of disc area was between 1.36 and 3.00 mm^2 in the current population if the normal range is defined between the 2.5 and 97.5 percentiles. The mean value of the disc area in the present report tended to be greater than that in normal white subjects[13,14] but smaller than that in normal black subjects.[17]

The characteristics of optic discs are usually well correlated between right and left eyes in each subject. One of the established criteria for diagnosing glaucoma in population-based studies, such as "difference of the vertical cup-to-disc ratio is 0.2 or more between both eyes,"[23,31–34] is based on the inter-eye similarity in optic disc shape in normal eyes. In previous studies, one study of 551 normal Turkish subjects found no significant inter-eye differences in HRT parameters,[20] whereas other studies on normal white subjects reported significant inter-eye differences in some HRT parameters, although the differences were small.[13,35,36] In the present report, all HRT parameters were strongly or moderately correlated between right and left eyes and no apparently significant inter-eye difference was found as a whole in all parameters except rim volume and height variation contour (Table 1 [available at http://aaojournal.org]). However, the absolute inter-eye differences in some parameters were not as small as clinically ignorable. For example, absolute inter-eye difference in cup-to-disc area ratio (0.07) was equivalent to 30% of the bilateral mean (0.23) of the parameter. Thus, the current results indicate that inter-eye difference in HRT parameters is not always small enough in each individual and that it cannot be adopted as a useful diagnostic tool in detecting disc pathology, especially among subjects with large optic discs because the absolute inter-eye difference was positively correlated with the optic disc size.

Several studies have reported significant gender-related differences in HRT parameters.[13–15,20,22] In normal subjects of various races, Tsai et al.,[15] using analysis of variance, found that women had a significantly greater rim volume and that men had significantly greater cup area, cup-to-disc area ratio, cup volume, and cup-to-disc ratio. In normal Turkish subjects, Durukan et al.,[20] using the *t* test, found that women had significantly greater height variation contour, mean RNFL thickness, and RNFL cross-sectional area. In normal white subjects, Hermann et al.[13] and Vernon et al.,[14] using the Mann-Whitney test, found that the women had significantly greater rim volume, mean RNFL thickness, and RNFL cross-sectional area. In Japan, Uchida et al.,[22] using the Mann-Whitney test, found that men had significantly greater disc area. However, none of these investigators adjusted for other important potential confounders such as age, height, and refraction using multiple regression analysis. In the present report, some HRT parameters were significantly different between male and female subjects using unpaired *t* test (Table 2), but the significant differences diminished after adjusting for the potential confounders using multiple regression analysis (Tables 4 and 5 [available at http://aaojournal.org]). Thus, gender itself is not thought to influence HRT parameters.

Between age and optic disc characteristics, several investigators observed significant association,[20–22,37–39] whereas others did not.[13,14,16,40,41] In normal white subjects, Hermann et al.,[13] using HRT, reported that although the disc area and mean RNFL thickness were smaller in older subjects (age, 52–70 years) than in younger subjects (35–40 years), no significant differences were noted. Vernon et al.[14] found no significant age-related differences in HRT parameters in normal white subjects, although rim and RNFL-related parameters tended to decrease with age. In contrast, although they were hospital-based studies and the numbers of subjects were not sufficiently large, one study of normal Japanese subjects found that mean RNFL thickness and RNFL cross-sectional area significantly decreased with in-

creasing age,[21] and another study found that rim volume, height variation contour, mean RNFL thickness, and RNFL cross-sectional area significantly decreased with increasing age and that cup shape measure significantly increased with increasing age.[22] In the present report, several HRT parameters, including disc area, correlated with age in both crude and partial correlation analyses. Approximately one third of the study participants had to be excluded from the analysis of HRT data, and because there was significant difference in age between the included and excluded subjects, the association of age with HRT parameters in the included subjects should be interpreted with caution. For example, the association between older age and smaller disc area may be attributable to the cohort effect than to the longitudinal effect because disc size is supposed to be unchanged throughout lifetime. However, this significant correlation between age and some HRT parameters indicates the importance of adjusting for age as a possible confounder in multiple regression analyses in the current subjects. After adjusting for disc area and the other potential confounders, rim area, rim volume, height variation contour, mean RNFL thickness, and RNFL cross-sectional area significantly decreased with increasing age, whereas cup area, cup-to-disc area ratio, and cup shape measure significantly increased with increasing age (Table 5 [available at http://aaojournal.org]). Our findings are consistent with those of the above previous studies of normal Japanese subjects. If age-related decrease in nerve fibers exists,[42–45] it is possible that HRT parameters that reflect the amount of nerve fibers may slightly decrease with increasing age.

In the present report, partial correlation analyses showed that disc area was not correlated with height, whereas some of the other HRT parameters were significantly correlated with height (Tables 4 and 5 [available at http://aaojournal.org]). After adjusting for the potential confounders, with increasing height, cup-related parameters weakly but significantly increased, whereas rim-related parameters weakly but significantly decreased. In contrast with our findings, the investigators of the Rotterdam Study, using image analysis of stereoscopic optic disc photographs, found no significant height-related differences in cup area and cup-to-disc area ratio.[41] Although the reasons for the discrepancy are unclear, racial differences and differences in methods of evaluating optic disc morphology are at least partially responsible.

In the present report of normal subjects (spherical refraction $\leq \pm 5$D and cylinder correction $\leq \pm 3$ D), both crude and partial correlation analyses showed that several HRT parameters weakly correlated with refractive error (Tables 3, 4, and 5 [available at http://aaojournal.org]). After adjusting for the potential confounders, disc area significantly decreased with an increase in myopia (Table 4 [available at http://aaojournal.org]). After adjusting for disc area and the other potential confounders, rim volume, height variation contour, mean RNFL thickness, and RNFL cross-sectional area significantly increased with an increase in myopia (Table 5 [available at http://aaojournal.org]). Some studies showed a significant influence of refractive errors on HRT parameters.[15,21] Tsai et al.[15] found that rim volume significantly increased with an increase in myopia in normal subjects of various races (refractive error between −6 and +3 D). Nakamura et al.[21] found that mean cup depth and maximum cup depth significantly increased with an increase in myopia in a relatively small sample of normal Japanese subjects (77 subjects, refractive error between −5 and +4.13 D). In contrast, Bowd et al.[38] and Durukan et al.[20] found no significant association between refractive error and HRT parameters in normal white subjects (refractive error $\leq \pm 5$ D) and normal Turkish subjects (refractive error between −4.75 and +4.25 D), respectively. Although the reasons for the differences among these studies and our study, are unclear, differences in sample sizes, subject characteristics, including age, refractive errors, and races, or methods of analyses might have affected the results.

Many studies have reported a significant effect of optic disc size on optic disc characteristics.[13–16,20–22,37,38,40,41] However, in normal Turkish subjects, Durukan et al.[20] found cup shape measure and height variation contour to be independent of disc area. In normal white subjects, Vernon et al.[14] found height variation contour to be the only parameter independent of disc area. Two previous studies of normal Japanese subjects using HRT also found height variation contour to be independent of disc area.[21,22] In the present report, all HRT parameters except height variation contour moderately or weakly correlated with disc area with P values of ≤ 0.001 in both crude and partial correlation analyses (Tables 5 and 6 [available at http://aaojournal.org]). Our findings are consistent with those of previous studies in that height variation contour, which is the height difference between the most elevated and most depressed points of the contour line, is independent of or minimally affected by optic disc size.[14,20–22] On the other hand, as in previous studies,[13–15,20–22,37,38,40] many cup, rim, or RNFL-related HRT parameters were closely influenced by optic disc size, suggesting that optic disc size should be considered in evaluating these parameters.

A recent study reported a significant association between systemic blood pressure and some of the HRT parameters in 232 Greek patients without glaucoma.[46] Topouzis et al[46] found a significant association of lower diastolic blood pressure with increased cup area and decreased rim area in multiple regression analysis. However, Jonas and Gründler[47] analyzed stereo optic disc photographs of 167 normal white subjects and found no significant influence of systemic hypertension on optic disc structure, including disc area and rim area. The present report on normal Japanese subjects did not find a significant association of systemic blood pressure with HRT parameters after adjusting for the possible confounders (Tables 4 and 5 [available at http://aaojournal.org]). Although the true reasons for these discrepancies are hard to be determined, differences in races and blood pressure itself between the studies may be possible explanations.

In the present report, weak but significant correlations between higher IOP and greater cup-related parameters were found in multiple regression analyses including disc area as an independent variable (Table 5). A similar relationship was found in the Blue Mountains Eye Study using optic disc photographs.[48] Investigators of the Beijing Eye Study also reported that rim area evaluated with optic disc photographs was significantly smaller in eyes with IOP >21 mmHg than those with IOP ≤21 mmHg, although, for the